Cell Injury, Repair, Aging and Apoptosis

Age-Related Changes in Pericellular Hyaluronan Organization Leads to Impaired Dermal Fibroblast to Myofibroblast Differentiation

Russell M.L. Simpson,* Soma Meran,*
David Thomas,[†] Philip Stephens,[†]
Timothy Bowen,* Robert Steadman,* and
Aled Phillips*

From the Institute of Nephrology,* School of Medicine, and Department of Oral Surgery,[†] School of Dentistry, Cardiff Institute of Tissue Engineering and Repair, Cardiff University Heath Park, Cardiff, United Kingdom

We have previously demonstrated that transforming growth factor-β1 (TGF-β1)-mediated fibroblast-myofibroblast differentiation is associated with accumulation of a hyaluronan (HA) pericellular coat. The current study demonstrates failure of fibroblast-myofibroblast differentiation associated with *in vitro* aging. This is associated with attenuation of numerous TGF-β1-dependent responses, including HA synthesis and induction of the HA synthase enzyme HAS2 and the hyaladherin tumor necrosis factor-α-stimulated gene 6 (TSG-6), which led to an age-related defect in pericellular HA coat assembly. Inhibition of HAS2-dependent HA synthesis by gene silencing, removal of the HA coat by hyaluronidase digestion, or gene silencing of TSG-6 or cell surface receptor CD44 led to abrogation of TGF-β1-dependent induction of α-smooth muscle actin in "young" cells. This result supports the importance of HAS2-dependent HA synthesis and the HA coat during phenotypic activation. Interleukin-1β stimulation, however, failed to promote phenotypic conversion despite coat formation. A return to basal levels of HA synthesis in aged cells by HAS2 overexpression restored TGF-β1-dependent induction of TSG-6 and pericellular HA coat assembly. However, this did not lead to the acquisition of a myofibroblast phenotype. Coordinated induction of HAS2 and TSG-6 facilitation of pericellular HA coat assembly is necessary for TGF-β1-dependent activation of fibroblasts, and both components of this response are impaired with *in vitro* aging. In conclusion, the HA pericellular coat is integral but not sufficient to correct for the age-dependent defect in phe-

notypic conversion. *(Am J Pathol 2009, 175:1915–1928; DOI: 10.2353/ajpath.2009.090045)*

Chronic skin wounds represent a major, often unrecognized, cause of distress and disability in the elderly population and have been estimated to affect 4% of the UK population older than 65. The morbidity associated with this impaired wound healing is estimated to cost the health service in excess of £1 billion annually in the UK[1] and $9 billion in the USA.[2] This amount will grow with the increasing age of the population.

Wound healing regardless of the etiology of the wound involves overlapping patterns of events including coagulation, inflammation, epithelialization, formation of granulation tissue, and remodeling of the matrix and tissue. Fibroblasts are central to the wound-healing process and when activated, they undergo a number of phenotypic transitions and eventually acquire a contractile "myofibroblastic" phenotype characterized by the expression of α-smooth muscle actin (α-SMA).[3] These myofibroblasts are responsible for closure of wounds and for the formation of the collagen-rich scar. In addition, their presence in tissues has been established as a marker of progressive fibrosis.[4,5] The cytokine transforming growth factor-β1 (TGF-β1) is recognized as a mediator of wound healing and its aberrant expression has also been widely implicated in progressive tissue fibrosis.[4,6,7] In addition to its direct effect on extracellular matrix turnover, it is known to drive fibroblast-myofibroblast differentiation and is capable of up-regulating α-SMA in fibroblasts both *in vitro* and *in vivo*.[8,9] Deficits in the signal transduction responsiveness to TGF-β1 have been postulated to explain the

age-related defects in wound healing seen in the elderly population.[10]

Hyaluronan (HA) is a ubiquitous connective tissue glycosaminoglycan synthesized by HA synthase (HAS) enzymes, for which three vertebrate genes have been isolated and characterized (*HAS1, HAS2,* and *HAS3*).[11,12] It has a role in maintaining matrix stability and tissue hydration. It is known to play a major role in regulating cell-cell adhesion,[13] migration,[14–16] differentiation,[17] and proliferation[18,19] and therefore plays an important role in wound healing. In addition, it is involved in mediating cellular responses to TGF-β1. For example, our recent studies in epithelial cells have demonstrated that HA modulates TGF-β1 signaling after interaction with its receptor, CD44.[20,21]

We have demonstrated previously that phenotypic conversion of fibroblasts to myofibroblasts is associated with major changes in the production and metabolism of HA.[22] Specifically they have been shown to accumulate larger amounts of intracellular and extracellular HA and assemble larger HA pericellular matrices. Furthermore, we demonstrated that HA plays a pivotal role in regulating TGF-β1-driven cellular differentiation in that it facilitates the fibroblast-myofibroblast transition.[23,24]

Fibroblasts have distinct phenotypes depending on the site from which they are isolated. Using a library of patient-matched oral and dermal fibroblasts we previously demonstrated the relationship between generation of HA and site-specific phenotypic variation.[23,24] An *in vitro* aging model based on cell senescence was described previously and validated as a model of age-related alterations in human aortic smooth muscle cell function.[25,26] Similarly alterations in fibroblast function in an *in vitro* model of aging have demonstrated the validity of this model in terms of *in vivo* age-related alterations in fibroblast motility and mitogenesis, which are associated with age-dependent impaired wound healing.[27,28] The aim of the work in this article was to understand the age-related regulation of HA generation, using this validated *in vitro* aging model, and determine how this regulation may contribute to age-related impaired wound healing.

Materials and Methods

Materials

All reagents were from Sigma-Aldridge (Poole, Dorset, UK) unless otherwise stated. PCR and quantitative PCR (QPCR) reagents and primers were purchased from Invitrogen (Paisley, UK) and Applied Biosystems (Cheshire, UK).

Cell Culture

All experiments were performed with dermal fibroblasts obtained by biopsy from consenting adults undergoing routine minor surgery. Ethical approval for the biopsies was obtained from the South East Wales Research Ethics Committee. The cells were isolated and characterized as described previously[23,24,29] and cultured in Dulbecco's modified Eagle's medium supplemented with L-glutamine (2 mmol/L), 100 units/ml penicillin and 100 μg/ml streptomycin, and 10% fetal bovine serum (FBS) (Biological Industries Ltd., Cumbernauld, UK). The cultures were maintained at 37°C in a humidified incubator in an atmosphere of 5% CO_2, and fresh growth medium was added to the cells every 3 to 4 days. At 90% confluence, fibroblasts were trypsinized and reseeded at the ratio of 1:3. At each passage, the total number of viable cells was determined by direct counting using a hemocytometer. The effect of aging was examined using a previously characterized and validated model of *in vitro* aging,[25] which has been demonstrated in a fibroblast model to have applicability to *in vivo* aging.[27] Population doubling levels (PDLs) were calculated as follows: PDL = [$\log_{10}$ (total cells harvested at passage $-$ $\log_{10}$(total cells reseeded)]/$\log_{10}$(2).[30] Cumulative population doubling levels were calculated by adding the derived increase to the previous PDL, and fibroblast populations were cultured until senescence, which varied for each patient, occurring at PDL 46 to 70. In the experiments, 10 to 15 PDL and 25 to 35 PDL were used and are referred to as young and aged dermal fibroblasts, respectively. The cells were incubated in serum-free medium for 48 hours before use in experiments, and all experiments were done under serum-free conditions unless otherwise stated.

Immunocytochemistry

Cells were grown to 70% confluence in eight-well Permanox chamber slides. The culture medium was removed, and the cells washed with sterile PBS. For immunostaining the cells were fixed in acetone-methanol (1:1, v/v) for 5 minutes at room temperature. After fixation, slides were blocked with 5% bovine serum albumin for 20 minutes before a further washing step with PBS. Subsequently the slides were incubated with murine monoclonal anti-α-SMA clone 1A4, diluted in 0.1% bovine serum albumin-PBS (final dilution 1:30) for 2 hours at room temperature. After a further washing step, slides were incubated with fluorescein isothiocyanate-rabbit anti-mouse IgG (DAKO, Cambridgeshire, UK) diluted 1:50 in 0.1% bovine serum albumin-PBS for 1 hour at room temperature. Cells were then mounted and analyzed by fluorescent microscopy.

Quantitative PCR

Young and aged dermal fibroblasts were grown to confluence in 35-mm dishes and washed with PBS before lysis with TRI Reagent and RNA purification according to the manufacturer's protocol. One microgram of total RNA was retrotranscribed using High Capacity cDNA Reverse Transcription Kits according to the manufacturer's protocol. These use the random primer method for initiating cDNA synthesis. As a negative control RT was performed with sterile H_2O replacing the RNA sample. Quantitative PCR was performed using the 7900HT Fast Real-Time PCR System from Applied Biosystems using TaqMan

Universal PCR Master Mix (Applied Biosystems) following the manufacturer's instructions. The following TaqMan gene expression assays were used: CD44 (HS00153304_m1, HAS2 (HS0019343_m1), tumor necrosis factor-α-stimulated gene 6 (TSG-6) (HS00200180_m1), and α-SMA (HS00426835_g1). PCR was performed in a final volume of 20 μl/sample (1 μl of RT product, 1 μl of target gene primers and probe, 10 μl of TaqMan Universal PCR Master Mix, and 8 μl of sterile H_2O). Amplification was performed using a cycle of 95°C for 1 second and 60°C for 20 seconds for 40 cycles. As a negative control, PCR was performed with sterile H_2O replacing the cDNA sample. PCR was simultaneously done for ribosomal RNA (primers and probe commercially designed and purchased from Applied Biosciences) as a standard reference gene. The comparative C_T method (threshold cycle where amplification is in the linear range of the amplification curve) was used for relative quantification of gene expression. The C_T for the standard reference gene (ribosomal RNA) was subtracted from the target gene C_T to obtain the ΔC_T (dC_T). The mean dC_T for similar samples were then calculated. The expression of the target gene in experimental samples relative to expression in control samples was then calculated using the formula, $2^{-(dCT(1)-dCT(2))}$, where: $dC_T(1)$ is the mean dC_T calculated for the experimental samples and $dC_T(2)$ is the mean dC_T calculated for the control samples.

Generation of HAS2 Overexpressing Clone

HAS2 open reading frame was a gift from Dr. Andrew Spicer (Texas A&M University, College Station, TX). Standard PCR was performed to generate the ORF using *Pfx50* DNA polymerase (Invitrogen) to increase the fidelity of the PCR product. The primers used in the reaction include sites for the restriction enzymes KpnI and NotI. The open reading frame was inserted into the vector (pCR3.1) using a standard ligation reaction with Promega T4 DNA ligase. Amplification of the cloned vector was performed via bacterial transformation (JM109 competent *Escherichia coli*, Promega, Madison, WI). The integrity and orientation of the HAS2 open reading frame was confirmed by restriction enzyme digestion (KpnI and NotI).

Transient transfection was performed with the aid of Nucleofector technology (Amaxa Biosystems, Gaithersburg, MD) in accordance with the manufacturer's protocol for transfection of primary mammalian fibroblasts. Fibroblasts were grown to 70% confluence in T75 flasks. The medium was then removed, and the cells were harvested by trypsinization (solution containing 0.05% trypsin and 0.53 mmol/L EDTA). Once the cells detached, the resulting cell suspension was treated with an equal volume of FBS to neutralize the protease activity. Cell counting was performed using a hemocytometer, and cell numbers were adjusted to a final concentration of 0.5 $\times$ 10^6 cells/ml. The cells were then centrifuged (100 $\times$ *g* for 10 minutes), and the resulting pellet was resuspended in Basic Nucleofector solution (Amaxa Biosciences). The cells were transfected either with HAS2-

pCR3.1 or pCR3.1 alone (mock transfection). The concentration we used was 100 μl of Basic Nucleofector solution to 1 μg of DNA. The solution was then transferred to an Amaxa-certified cuvette and placed in the Nucleofector. Nucleofection was performed for 5 seconds according to the pre-specified program designed for mammalian fibroblasts, and the cells were subsequently transferred to either 35-mm dishes or eight-well Permanox chamber slides containing prewarmed medium supplemented with 10% FBS. pmaxGFP (green fluorescent protein) vector was used as a positive control. Two negative controls were performed: 0.5 $\times$ 10^6 cells in 100 μl of Basic Nucleofector solution containing 1 μg of DNA but without application of the program and 0.5 $\times$ 10^6 cells in 100 μl of Basic Nucleofector solution without DNA but with application of the program. The cells were incubated in medium supplemented with 10% FBS for 24 hours followed by a 24-hour incubation in serum-free medium before experimentation. GFP positivity in pmaxGFP-HAS2 cotransfected or pmaxGFP-mock cotransfected cells were used to visualize individual cells for HA coat analysis.

siRNA Transfection

Transient transfection of dermal fibroblasts was performed with specific siRNA nucleotides (Applied Biosystems) targeting HAS2 (56458), TSG-6 (139706), or CD44 (114068). Transfection was performed using Lipofectamine 2000 transfection reagent (Invitrogen) in accordance with the manufacturer's protocol. In brief, cells were grown to 50% confluence in antibiotic-free medium in either 12-well culture plates or 8-well Permanox chamber slides. Two microliters of transfection agent was diluted in 98 μl of Opti-MEM reduced growth medium (GIBCO, Carlsbad, CA) and left to incubate at room temperature for 5 minutes. The specific siRNA oligonucleotides were diluted in Opti-MEM reduced growth medium to give a final concentration of 20 μmol/L in a total volume of 100 μl. The transfection agent mix and siRNA mix were then combined and incubated at room temperature for a further 10 minutes. The newly formed transfection complexes (200 μl) were then added to cells and incubated at 37°C with 5% CO_2 for 24 hours in medium supplemented with 10% FBS followed by a 24-hour incubation in serum-free medium before experimentation. As a control, cells were transfected with negative control siRNA (a scrambled sequence that bears no homology to the human genome).

### Visualization of Pericellular HA by Particle Exclusion Assay

The exclusion of horse erythrocytes was used to visualize the HA pericellular coat. Formalized horse erythrocytes were washed in PBS and centrifuged at 1000 $\times$ *g* for 7 minutes at 4°C. The pellet was resuspended in serum-free medium at an approximate density of 1 $\times$ 10^8 erythrocytes/ml. One milliliter of this suspension was added to each 35-mm dish containing subconfluent cells and

swirled gently for even distribution. The dishes were incubated at 37°C for 15 minutes to allow the erythrocytes to settle around the cells. Control cells were incubated with 200 μg/ml bovine testicular hyaluronidase in serum-free medium for 30 minutes before the addition of formalized horse erythrocytes. On settling, the erythrocytes are excluded from zones around the cells with HA pericellular coats. These zones are viewed under the microscope as areas of erythrocyte exclusion. Zones of exclusion were visualized on a Zeiss Axiovert 135 inverted microscope. Because of the elongated shape of the cells, the exclusion zone at some areas of the cell was not visible. Therefore, the width of the exclusion zone was calculated at the widest point of the cell (usually the nucleus).

Analysis of ^{3}H-Radiolabeled HA

Cells were grown to full confluence in T75 flasks and growth-arrested for 48 hours in serum-free medium. The medium was then replaced with either serum-free medium alone or serum-free medium containing 10 ng/ml TGF-β1, and the incubations were continued for 72 hours. Metabolic labeling was then performed by incubation with 20 μCi/ml D-[^{3}H]glucosamine hydrochloride for 24 hours. The culture medium was then removed, and the cells were washed with PBS. The wash and medium were combined to form the conditioned medium extract. This was then treated with an equal volume of 200 μg/ml Pronase in 100 mmol/L Tris-HCl, pH 8.0, and 0.05% sodium azide for 24 hours. To remove any CD44-associated HA, the cells were treated with 10 μg/ml trypsin in PBS for 10 minutes at room temperature and designated the trypsin extract. This was then treated with an equal volume of 200 μg/ml Pronase for 24 hours. The cells remaining in the culture flask were incubated directly with 100 μg/ml Pronase for 24 hours. The supernatant was decanted and designated the cell extract. Each extract was passed over DEAE-Sephacel ion-exchange columns equilibrated with 8 mol/L urea in 20 mmol/L Bis-Tris buffer, pH 6, containing 0.2% Triton X-100. This process removed any low-molecular-weight peptides and unincorporated radiolabel. HA was eluted in 8 mol/l urea buffer containing 0.3 mol/l NaCl. Each sample was split into two, and the HA was precipitated with 3 volumes of 1% potassium acetate in 95% ethanol in the presence of 50 μg/ml of each HA, heparin, and chondroitin sulfate as coprecipitants. The first half of each sample was resuspended in 500 μl of 4 mol/L guanidine buffer and analyzed on a Sephacryl S-500 column equilibrated with 4 mol/L guanidine buffer. To confirm that the chromatography profile generated was the result of radiolabeled HA, the second half of each sample was digested at 37°C overnight with 1 unit of *Streptomyces hyalurolyticus* hyaluronidase (ICN Pharmaceuticals Ltd., Hampshire, UK) in 200 μl of 20 mmol/L sodium acetate, pH 6, containing 0.05% sodium azide and 0.15 mol/L sodium chloride. The sample was then mixed with an equal volume of 4 mol/L guanidine buffer and analyzed on the same Sephacryl S-500 column equilibrated with 4 mol/L guanidine buffer. To produce the chromatography profile, the ^{3}H activity for

each half of the sample was normalized and corrected for dilution, and then the hyaluronidase-resistant counts were subtracted. The chromatography profiles only depict hyaluronidase-sensitive activity in each fraction plot-

In vitro aging
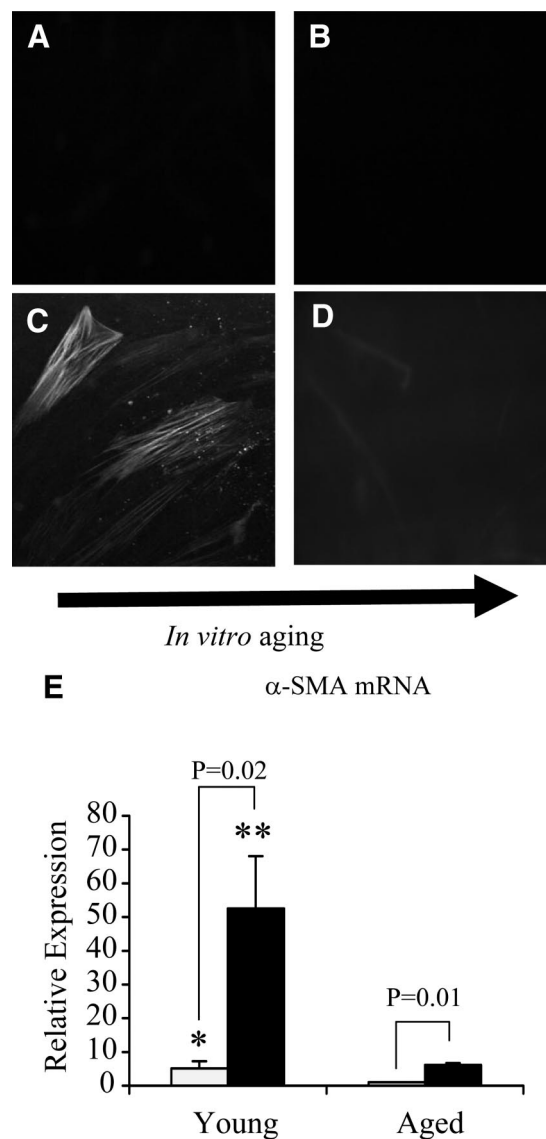
Figure 1. Immunohistochemical analysis of TGF-β1-dependent α-SMA expression in aging fibroblasts. Monolayers of patient-matched young (**A** and **C**) and aged (**B** and **D**) dermal fibroblasts were growth-arrested in serum-free medium for 48 hours. The medium was then replaced with either serum-free medium alone (**A** and **B**) or serum-free medium containing 10 ng/ml TGF-β1 (**C** and **D**) for 72 hours. The cells were then fixed and stained for α-SMA, as described in *Materials and Methods*. The cells were then mounted in Vectashield fluorescent mountant and viewed under UV light. All results shown are representative of dermal fibroblasts from three patient donors. Original magnification, ×100. **E:** In a parallel experiment expression of α-SMA mRNA was quantified by QPCR. Confluent monolayers of patient-matched young and aged dermal fibroblasts were growth-arrested in serum-free medium for 48 hours, before addition of either serum-free medium alone (white bar) or serum-free medium containing 10 ng/ml TGF-β1 (black bar) for 72 hours. Total mRNA was extracted, and α-SMA expression was assessed by RT-QPCR. Ribosomal RNA expression was used as an endogenous control, and gene expression was assessed relative to control (unstimulated) aged fibroblasts. The comparative C_T method was used for relative quantification of gene expression, and the results represent the mean ± SE of dermal fibroblasts from nine individual experiments with cells isolated from three patient donors. Statistical analysis was performed by the Student's *t*-test: *$P < 0.05$; **$P < 0.01$, compared with aged cells.
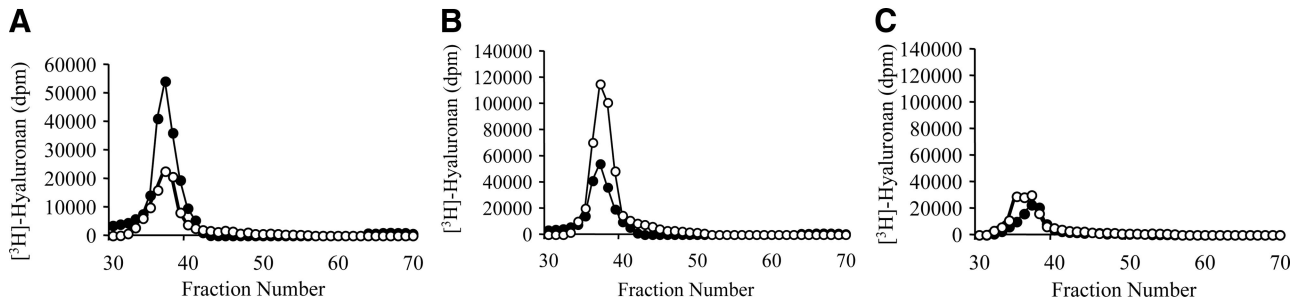
Figure 2. Age-dependent effect on HA assessed by size exclusion chromatography. Confluent monolayers of patient-matched young and aged dermal fibroblasts were growth arrested in serum-free medium for 48 hours. The medium was removed and replaced with either serum-free medium alone or with serum-free medium containing 10 ng/ml of TGF-β1 for 72 hours. Cells were subsequently labeled for 24 hours with 20 μCi/ml [^{3}H]glucosamine. The radiolabeled HA was isolated from the conditioned medium and subjected to size exclusion chromatography on a Sephacryl S500 column. **A:** Size exclusion chromatography profile of HA purified from resting (nonstimualted) young (closed circles) and aged (open circles) fibroblasts. **B** and **C:** Size exclusion chromatography profile of HA purified from young (**B**) and aged (**C**) dermal fibroblasts in the presence (open circles) or absence (closed circles) of TGF-β1. All results shown are representative of dermal fibroblasts isolated from at least two separate donors.

ted against fraction number. The column was calibrated with [^{3}H]glucosamine hydrochloride, M_r 215; [^{35}S]chondroitin sulfate glycosaminoglycans, M_r 25 $\times$ 10^3; decorin, M_r 10 $\times$ 10^4; and [^{35}S]versican, M_r 1.3 $\times$ 10^6.

Determination of HA Concentration

Cells were grown to confluence in 35-mm dishes, and the HA concentration in the cell culture supernatant was determined using a commercially available enzyme-linked HA binding protein assay (HA "Chugai" quantitative test kit, Congenix, Petersborough, UK). The assay used microwells coated with a highly specific HA-binding protein (HABP) from bovine cartilage to capture HA and an enzyme-conjugated version of HABP to detect and measure HA in the samples. In brief, diluted samples and HA reference solutions were incubated in HABP-coated microwells allowing binding of the HA in the samples to the immobilized HABP. The wells were then washed, and HABP conjugated with horseradish peroxidase was added to the wells forming complexes with bound HA. After a second washing step, a chromogenic substrate (3,3′,5,5′-tetramethylbenzidine/H$_2$O$_2$) was added to develop a colored reaction. Stopping solution was added to the wells, and the intensity of the resulting color was measured in optical density units using a spectrophotometer at 450 nm. HA concentrations were calculated by comparing the absorbance of the sample against a reference curve prepared from the reagent blank and five HA reference solutions (50, 100, 200, 500, and 800 ng/ml) included in the kit. The assay is sensitive to 10 ng/ml, with no cross-reactivity with other glycosaminoglycan compounds.

Statistical Analysis

All experiments were performed at least in triplicate for individual patient donors. All values are provided as means $\pm$ SE. Comparisons were performed using unpaired Student's *t*-tests. For multiple variables one-way analysis of variance was used for global comparison followed by Tukey's honestly significant difference method for pairwise comparison. Probability values of

$P < 0.05$ were considered to indicate a significant difference.

Results

In Vitro Aging of Fibroblasts Is Associated with a Failure to Induce α-Smooth Muscle Actin

Fibroblasts were grown to confluence and serum-deprived for 48 hours before addition of recombinant TGF-β1 (10 ng/ml) for a further 72 hours. Under serum-free conditions, dermal fibroblasts at all *in vitro* ages were negative for α-SMA staining (Figure 1, A and B). Stimulation of young fibroblasts led to positive staining for α-SMA (Figure 1C). In contrast, addition of TGF-β1 to *in vitro* aged fibroblasts did not lead to detectable staining for α-SMA (Figure 1D). Quantitative PCR demonstrated that under unstimulated conditions young fibroblasts had significantly higher (~5 fold) α-SMA mRNA ex-
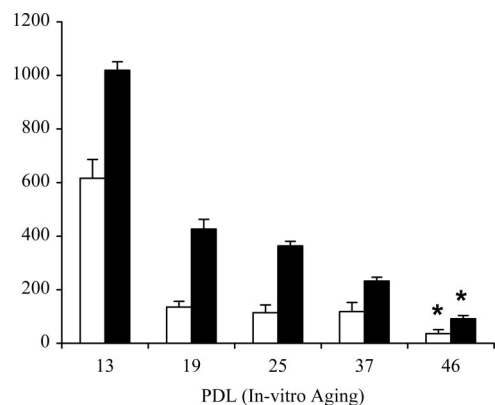
Figure 3. Effect of *in vitro* aging on extracellular HA generation. At the indicated PDL, confluent monolayers of dermal fibroblasts were growth-arrested in serum-free medium for 48 hours. The medium was then replaced with either serum-free medium alone (white bars) or serum-free medium containing 10 ng/ml TGF-β1 (black bars) for 72 hours. HA concentration in the culture medium was quantified by ELISA. Data represent the mean $\pm$ SE from six separate experiments using cells isolated from one donor. Statistical analysis was performed using analysis of variance to show global differences between PDLs for basal ($P = 1.1E-09$) and TGF-β1 ($P = 1.9E-19$) conditions, followed by Tukey's honestly significant difference post hoc test analysis: *$P < 0.001$ compared with PDL 13.

pression than patient-matched aged fibroblasts (Figure 1E). After TGF-β1 stimulation, both young and aged dermal fibroblasts up-regulated α-SMA expression. Young dermal fibroblasts, however, showed a median
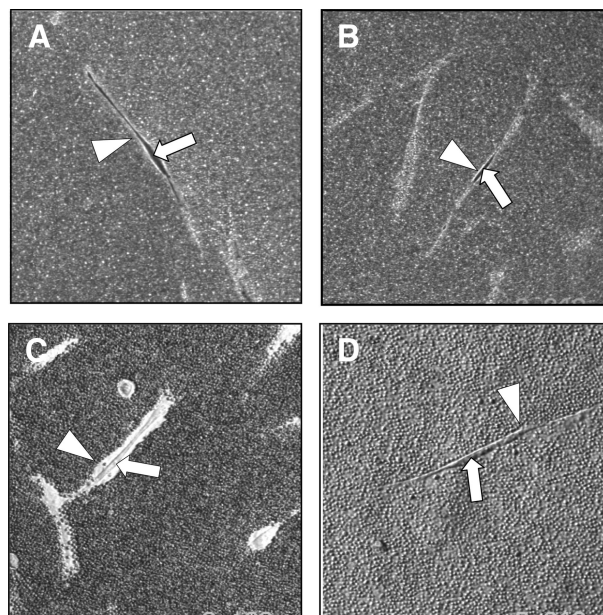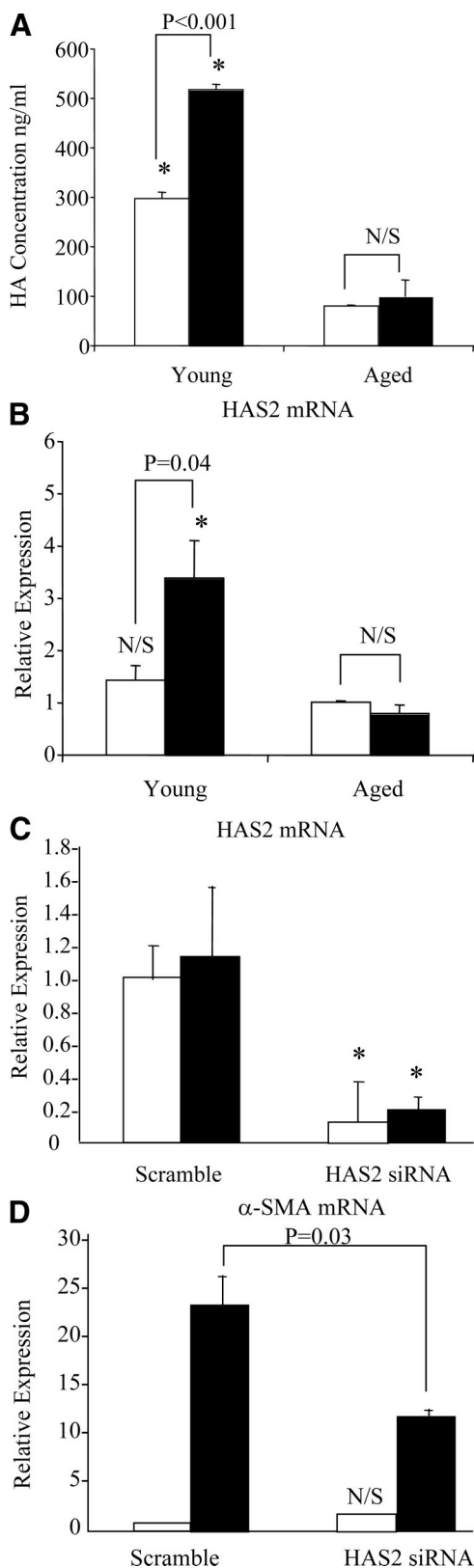
Figure 5. Effect of aging on HA pericellular coat assembly. Subconfluent layers of young (**A** and **C**) and aged (**B** and **D**) dermal fibroblasts were growth-arrested in serum-free medium for 48 hours. The medium was then replaced with either serum-free medium alone (**A** and **B**) or with 10 ng/ml TGF-β1 (**C** and **D**) for 72 hours. Formalized horse erythrocytes were then added as described in *Materials and Methods* to visualize the HA pericellular coat. **Arrows** indicate the cell body; **arrowheads** show the extent of the pericellular matrix. Results are representative of dermal fibroblasts from three patient donors. Original magnification, ×200.

10-fold increase in α-SMA expression compared with a median of only sixfold increase in aged dermal fibroblasts in response to the same concentration and duration of TGF-β1 stimulation. Moreover, a direct comparison between cell populations demonstrated that TGF-β1 induced α-SMA expression was down-regulated by 8.5-fold in aged fibroblasts compared with that in patient-matched young fibroblasts.

Figure 4. Effect of age on HAS2 mRNA expression and its involvement in TGF-β1-dependent fibroblast activation. **A** and **B:** Confluent monolayers of patient-matched young and aged dermal fibroblasts were growth-arrested in serum-free medium for 48 hours. The medium was then replaced with either serum-free medium alone (white bars) or serum-free medium containing 10 ng/ml TGF-β1 (black bars), and the incubations were continued for 72 hours. HA secreted into the culture medium was quantified by ELISA. After removal of the culture medium, total mRNA was extracted and cDNA prepared as described in *Materials and Methods.* HAS2 expression was assessed by RT-QPCR. Ribosomal RNA expression was used as an endogenous control, and gene expression was assessed relative to control aged fibroblasts. The comparative C_T method was used for relative quantification of gene expression. Data are presented as the mean ± SE of six individual experiments using cells from two patient donors. Statistical analysis was performed by Student's *t*-test: #not significant; *$P < 0.01$, compared with aged cells. N/S, not significant. **C** and **D:** To further examine the role of HAS2, young dermal fibroblasts were transfected with HAS2 siRNA or scrambled oligonucleotide control (scramble) and incubated in medium supplemented with 10% FBS for 24 hours. The medium was then replaced with serum-free medium for a further 24 hours, before addition of serum-free medium alone (white bars) or serum-free medium containing 10 ng/ml TGF-β1 (black bars) for 72 hours. Total mRNA was extracted and HAS2 (**C**) and α-SMA (**D**) expression was assessed by RT-QPCR. Ribosomal RNA expression was used as an endogenous control, and gene expression was assessed relative to control scramble samples. The comparative C_T method was used for relative quantification of gene expression, and the results represent the mean ± SE of nine individual experiments using cells isolated from three different donors. Statistical analysis was performed by the Student's *t*-test: N/S, not significant; *$P < 0.01$, compared with scramble.

## Young Fibroblasts Generate More HA Than Aged Fibroblasts

Labeling of fibroblasts with [³H]glucosamine for 24 hours under serum-free conditions demonstrated that young fibroblasts have increased baseline synthesis of HA compared with that of donor-matched aged fibroblasts (Figure 2A). Analysis of HA by size exclusion chromatography indicated that there was at least 2.5-fold more HA present in the conditioned medium of young fibroblasts than in

aged fibroblasts. Young fibroblasts also had 3.5-fold more trypsin-accessible cell surface extract HA but had similar amounts of HA in the cell-associated extract compared with aged fibroblasts (data not shown). The majority of HA produced in each of these three compartments consisted of high-molecular-weight HA polysaccharides of greater than 1.5×10^6 Da in size. These findings were similar in both the young and aged cells.

The effect of TGF-β1 on HA synthesis was then assessed using both [³H]glucosamine labeling and an enzyme-linked immunosorbent assay. The chromatography profiles from the conditioned medium of these cells demonstrated that young fibroblasts up-regulated HA generation in response to TGF-β1 stimulation (Figure 2B), whereas aged fibroblasts were resistant to up-regulation of HA in response to same dose and duration of TGF-β1 stimulation (Figure 2C). The chromatography profiles from the cell-associated extract and trypsin-accessible cell surface extract demonstrated a similar pattern (data not shown). These results were further confirmed by measurement of extracellular HA concentration in the conditioned medium using an enzyme-linked immunosorbent assay (ELISA), from cells at different PDLs (PDL 13 to 46). In this assay, there was a significant decrease in extracellular HA concentration between PDL 13 and PDL 46, under basal conditions ($P = 1.1E-09$, one-way analysis of variance; $P < 0.001$, Tukey's honestly significant difference post hoc test) and after TGF-β1 stimulation ($P = 1.9E-19$, one-way analysis of variance; $P < 0.001$ Tukey's honestly significant difference post hoc test) (Figure 3).

Reduced HA Generation Is Associated with a Blunted HAS2 Response

After growth arrest young and aged dermal fibroblasts were stimulated with TGF-β1. HA was quantified by ELISA, and in the same cells HAS2 mRNA was quantified by QPCR. As demonstrated previously there was an age-dependent decrease in HA concentration in the culture supernatant and also a decrease in TGF-β1-dependent stimulation of HA (Figure 4A). In the same cells there was a marked attenuation of TGF-β1-dependent stimulation of
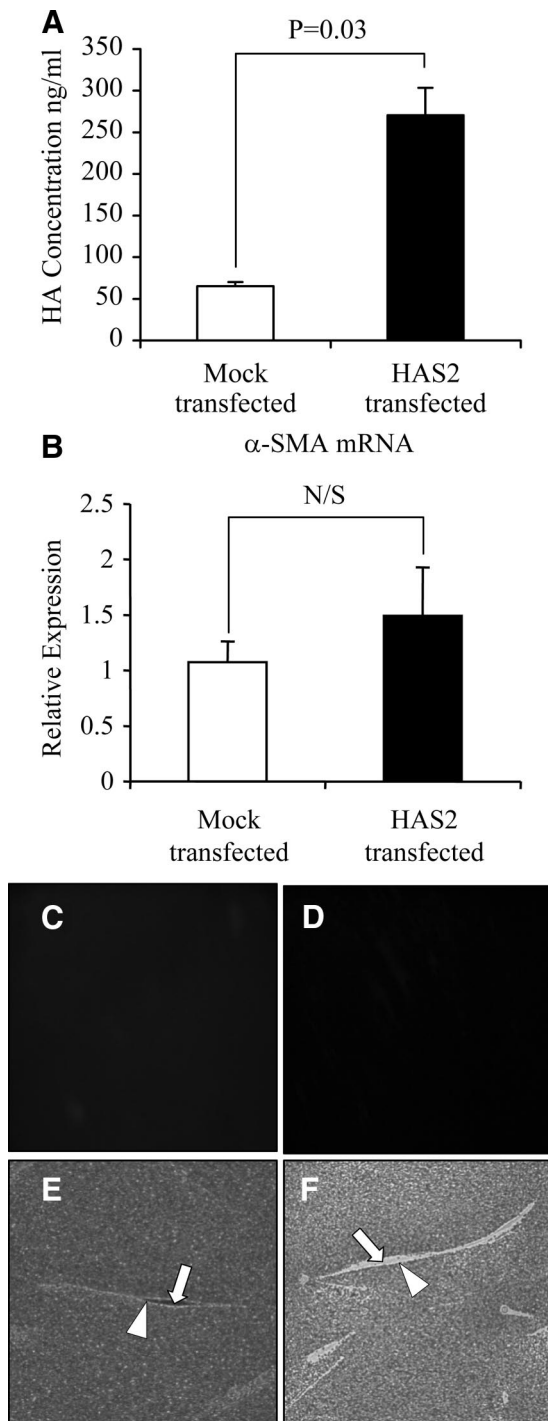
Figure 6. Overexpression of HAS2 in aged dermal fibroblasts. Aged dermal fibroblasts were transfected with either HAS2-pCR3.1 (HAS2 transfected) or pCR3.1 (Mock transfected). HA secreted into the culture medium 48 hours after transfection was quantified by ELISA (**A**). After removal of the culture medium, total mRNA was extracted. α-SMA expression was subsequently assessed by RT-QPCR (**B**). Ribosomal RNA expression was used as an endogenous control, and gene expression was assessed relative to mock transfected fibroblasts. The comparative C_T method was used for relative quantification of gene expression, and results represent the mean ± SE of dermal fibroblasts from nine separate experiments using cells isolated from three patient donors. Immunohistochemical analysis was performed to examine α-SMA protein expression on mock transfected (**C**) and HAS2-overexpressing (**D**) aged dermal fibroblasts 48 hours after transfection. The cells were then fixed and stained for α-SMA, mounted in Vectashield fluorescent mountant, and viewed under UV light. Original magnification, ×100. In parallel experiments, the HA pericellular coat was visualized. Forty-eight hours after transfection, formalized horse erythrocytes were added to mock-transfected (**E**) or HAS2-overexpressing (**F**) aged dermal fibroblasts as described in *Materials and Methods* to visualize the HA pericellular coat. **Arrows** indicate the cell body; **arrowheads** show the extent of the pericellular matrix. Results are representative of dermal fibroblasts from two patient donors. Original magnification, ×200.

HAS2 mRNA in the aged fibroblasts (Figure 4B). The importance of the HAS2 isoform of HA synthase was further examined by gene silencing of HAS2 in young cells. HAS2 siRNA transfection resulted in significant inhibition of HAS2 mRNA expression (Figure 4C) and abrogation of TGF-β1-dependent induction of α-SMA (Figure 4D).

Aging Is Associated with Loss of TGF-β1-Dependent Pericellular Coat Assembly

HA accumulation can be assessed using the exclusion of formalized erythrocytes. In this assay erythrocytes are excluded from the cell membrane of the fibroblasts by the large size and negative charge of any pericellular HA present as observed under the microscope as a zone of erythrocyte exclusion surrounding the cells. Previously we demonstrated that fibroblast to myofibroblast phenotypic conversion is associated with the formation of a HA pericellular coat. Consistent with this finding, unstimulated young or aged fibroblasts did not assemble a significant HA pericellular coat (Figure 5, A and B) whereas stimulation of young fibroblasts with TGF-β1 resulted in the formation of a notable coat (Figure 5C). In contrast, aged fibroblasts failed to assemble a HA pericellular coat after stimulation with TGF-β1 (Figure 5D). For each condition measurements of coat thickness were taken at the widest point of 10 randomly chosen cells from three separate experiments (three different patients). This gave a mean thickness for the young fibroblast coat of 2.99 $\pm$ 0.18 μm at baseline and 7.95 $\pm$ 0.39 μm after TGF-β1 stimulation ($P < 0.001$, unpaired t-test). For aged fibroblasts the mean coat thickness at baseline was 2.27 $\pm$ 0.16 μm and after TGF-β1 stimulation was 2.35 $\pm$ 0.21 μm ($P = 0.78$, unpaired t-test).

Overexpression of HAS2 Alone Does Not Generate a Pericellular Coat nor Alter the Fibroblast Phenotype

Because age-dependent loss of TGF-β1-induced pericellular coat assembly and the myofibroblast phenotype were associated with reduced HAS2 expression, we sought to examine the effect of overexpression of HAS2 on the phenotype of aged fibroblasts. Although overexpression of HAS2 in the aged fibroblast led to the expected increase in HA concentration in the culture supernatant as assessed by ELISA (Figure 6A), there was no significant change in α-SMA expression (Figure 6, B–D) nor in the pericellular HA coat assembly (Figure 6, E and F). For each condition, measurements of coat thickness were taken at the widest point of 15 randomly chosen cells from two separate patients. This gave a mean thickness for the aged mock-transfected fibroblast coat of 4.82 $\pm$ 0.31 μm and of 4.41 $\pm$ 0.42 μm in the aged fibroblast coat transfected to overexpress HAS2 ($P = 0.42$, unpaired t-test).
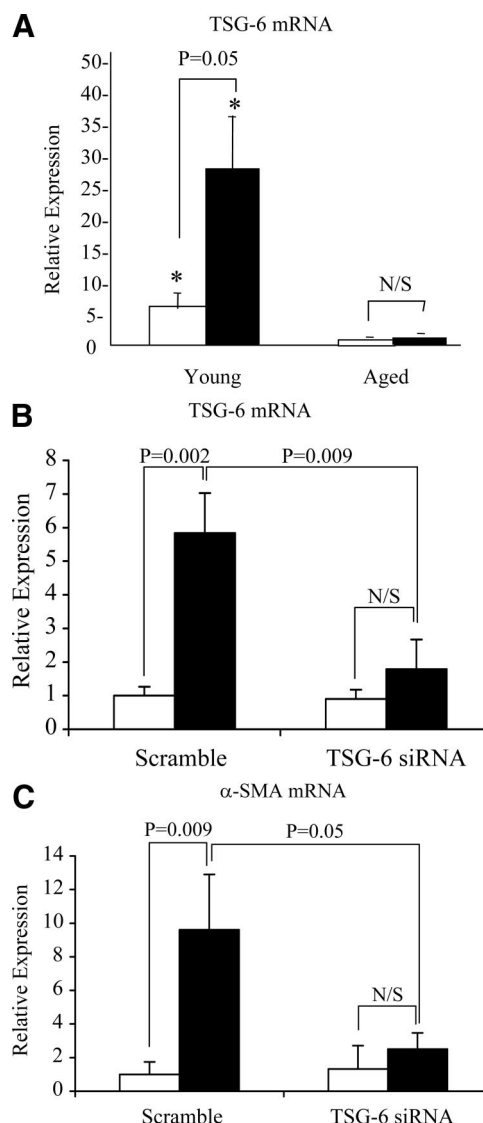
Figure 7. Involvement of TSG-6 in TGF-β1-dependent fibroblast activation. **A:** Confluent monolayers of patient-matched young and aged dermal fibroblasts were growth-arrested in serum-free medium for 48 hours. The medium was then replaced with either serum-free medium alone (white bars) or serum-free medium containing 10 ng/ml TGF-β1 (black bars), and the incubations were continued for 72 hours. Total mRNA was extracted, and cDNA was prepared as described under Materials and Methods. TSG-6 expression was assessed by RT-QPCR. Ribosomal RNA expression was used as an endogenous control, and gene expression was assessed relative to control aged fibroblasts. The comparative C_T method was used for relative quantification of gene expression. Data are presented as the mean $\pm$ SE of six individual experiments with cells isolated from two patient donors. Statistical analysis was performed by Student's t-test:*$P < 0.05$, compared with aged cells. N/S, not significant. **B** and **C:** To further examine the role of TSG-6, young dermal fibroblasts were transfected with TSG-6 siRNA or scrambled oligonucleotide control (scramble) and incubated in medium supplemented with 10% FBS for 24 hours. The medium was then replaced with serum-free medium for a further 24 hours, before addition of serum-free medium alone (white bars) or serum-free medium containing 10 ng/ml TGF-β1 (black bars) for 72 hours. Total mRNA was extracted and TSG-6 (**B**), and α-SMA (**C**) expression was assessed by RT-QPCR. Ribosomal RNA expression was used as an endogenous control, and gene expression was assessed relative to control scramble samples. The comparative C_T method was used for relative quantification of gene expression, and the results represent the mean $\pm$ SE of nine individual experiments using cells isolated from three different donors. Statistical analysis was performed by Student's t-test, and statistical significance was taken as $P < 0.05$. N/S, not significant.
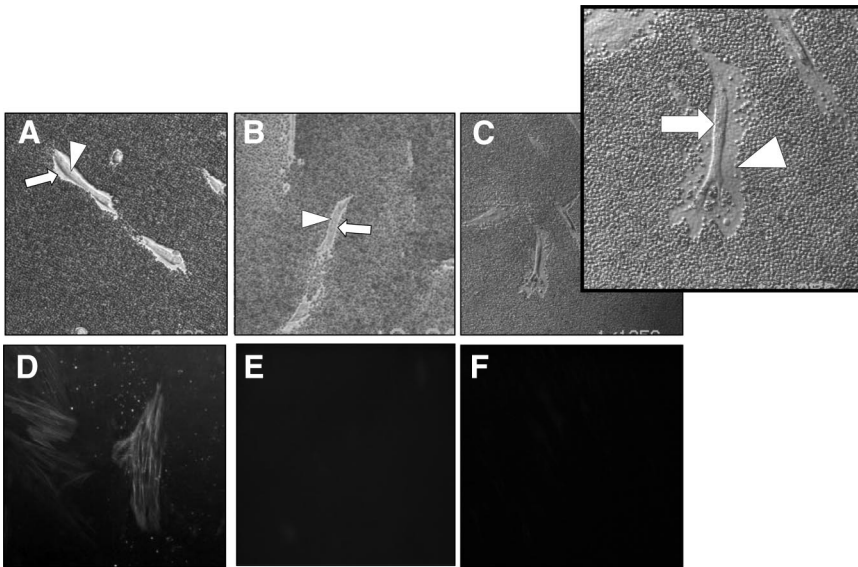
Figure 8. Effect of HAS2 overexpression on pericellular HA coat assembly and phenotype after TGF-β1 in aged dermal fibroblasts. Patient-matched young (**A** and **D**) and aged (**B, C, E,** and **F**) dermal fibroblasts were transfected either with pCR3.1 alone (**A, B, D,** and **E**) or HAS2-pCR3.1 (**C** and **F**). Forty-eight hours after transfection, cells were incubated in serum-free medium containing 10 ng/ml TGF-β1 for 72 hours. The pericellular HA coat (**A–C**) was visualized by addition of formalized horse erythrocytes. **Arrows** indicate the cell body; **arrowheads** show the extent of the pericellular matrix. Images are representative of dermal fibroblasts from three patient donors. Original magnification, ×200. After stimulation the cells were fixed, and α-SMA was visualized by immunohistochemistry (**D–F**). Slides were mounted in Vectashield fluorescent mountant and viewed under UV light. Original magnification, ×100.

TSG-6 Is a Key Regulator of Pericellular HA Assembly and Fibroblast Phenotype

The hyaladherin TSG-6 has been demonstrated to be an important mediator of HA pericellular coat assembly.[31–33] After growth arrest young and aged dermal fibroblasts were stimulated with TGF-β1, and TSG-6 mRNA was quantified by QPCR. In these experiments there was an age-dependent decrease in TSG-6 expression both at baseline and after TGF-β1 stimulation (Figure 7A). The functional importance of an age-dependent reduction in TSG-6 expression was subsequently examined by TSG-6 gene silencing using siRNA. After transfection with TSG-6 siRNA there was a marked inhibition in the effect of TGF-β1 on TSG-6 mRNA expression (Figure 7B). Abrogation of TGF-β1-dependent induction of TSG-6 mRNA expression was also associated with a failure of TGF-β1 to increase α-SMA in the young fibroblasts (Figure 7C). This result led us to hypothesize that assembly of the pericellular coat was dependent on both stimulation of HA via HAS2 and induction of TSG-6. To explore this hypothesis aged fibroblasts were transfected with HAS2 and subsequently stimulated with TGF-β1. In these experiments the combination of HAS2 overexpression and TGF-β1 stimulation restored the ability of the aged fibroblasts to form a pericellular HA coat as assessed by the exclusion of formalized erythrocytes (Figure 8, A–C). For each condition measurements of coat thickness were taken at the widest point of 10 randomly chosen cells from three separate experiments (three different patients). This gave a mean thickness for the aged mock-transfected fibroblast coat of 3.19 ± 0.27 μm and of 6.59 ± 0.41 μm in the aged fibroblasts transfected to overexpress HAS2 after TGF-β1 stimulation ($P < 0.001$, unpaired t-test). Transfection with HAS2 did not, however, restore TGF-β1 responsiveness in terms of the induction of α-SMA as assessed by immunocytochemical analysis (Figure 8, D–F) and QPCR (Figure 9A), suggesting a dissociation of pericellular coat formation and regulation of phenotype. In contrast and consistent with the

formation of the pericellular coat, overexpression of HAS2 and increased HA generation were associated with partial restoration of the induction of TSG-6 after stimulation with TGF-β1 in the aged fibroblasts (Figure 9B).

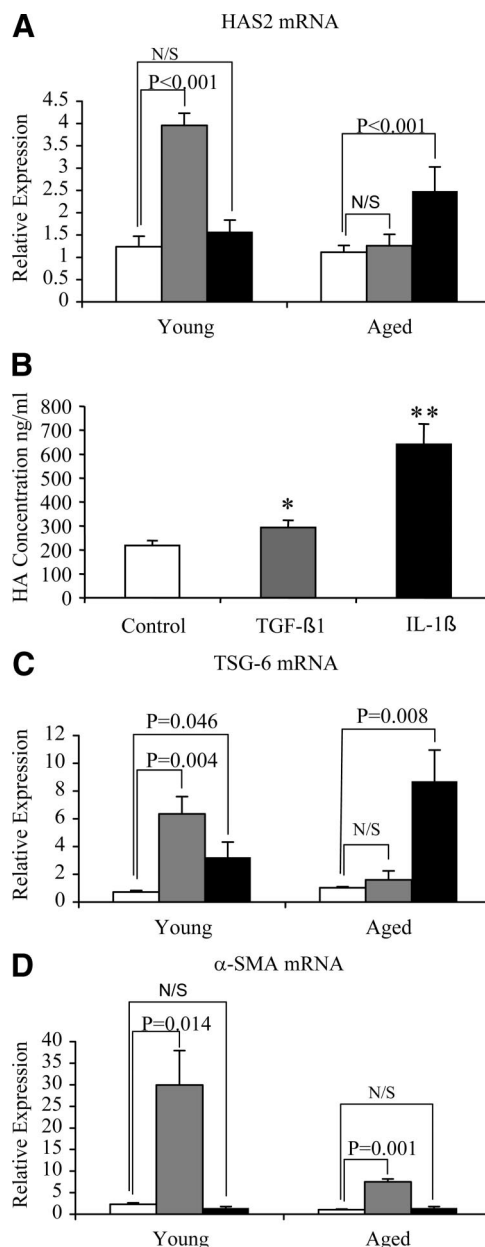## HAS2 Responsiveness Is Maintained in Aged Cells in Response to Interleukin-1β

Age-dependent regulation of HAS2 was further examined by stimulation with IL-1β. In contrast with TGF-β1 responsiveness that diminished with age, stimulation of aged cells (but not young cells) with IL-1β led to a significant induction of HAS2 gene expression (Figure 10A), and this was also associated with an increase in HA as assessed by ELISA (Figure 10B). In addition, TSG-6 induction was significant after addition of IL-1β in contrast to the blunted effect of TGF-β1 in the aged cells (Figure 10C). In contrast, stimulation with IL-1β, despite the alterations in HA-associated gene regulation, did not lead to any change in expression of α-SMA (Figure 10D). The increase in HAS2 associated with induction of the hyaladherin TSG-6 suggests that IL-1β stimulation may induce formation of a pericellular HA coat, and this was confirmed by visualization of the pericellular HA coat in young and aged cells (Figure 11, A–D). For each condition, measurements of coat thickness were taken at the widest point of 15 randomly chosen cells from two separate experiments (two different patients). These gave a mean thickness for the young fibroblast coat of 3.04 ± 0.19 μm at baseline and 8.25 ± 0.18 μm after IL-1β stimulation ($P < 0.001$, unpaired t-test). For aged fibroblasts the mean coat thickness at baseline was 3.15 ± 0.35 μm and after IL-1β stimulation was 7.95 ± 0.42 μm ($P = 0.001$, unpaired t-test). This finding suggests, therefore, that after IL-1β stimulation there is a dissociation of pericellular HA coat assembly and regulation of phenotype.

A   α-SMA mRNA

B   TSG-6 mRNA
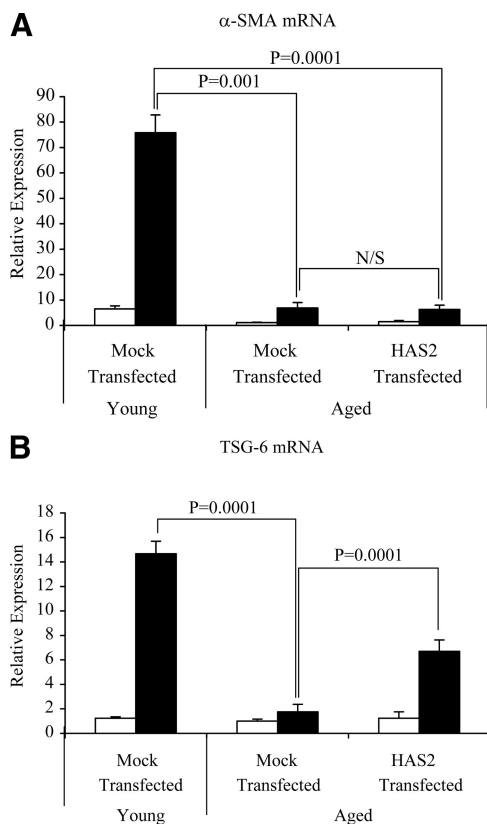
Figure 9. Effect of HAS2 overexpression on TGF-β1-dependent responses in aged dermal fibroblasts. Aged dermal fibroblasts were transfected either with HAS2-pCR3.1 or pCR3.1 alone (mock transfected). Parallel mock transfections were performed on patient-matched young dermal fibroblasts. Forty-eight hours after transfection, cells were incubated in either serum-free medium alone (white bars) or serum-free medium containing 10 ng/ml TGF-β1 (black bars) for 72 hours. α-SMA (**A**) and TSG-6 (**B**) mRNA expression was assessed by RT-QPCR. Ribosomal RNA expression was used as an endogenous control, and gene expression was assessed relative to control mock-transfected aged cells. The comparative C_T method was used for relative quantification of gene expression, and the results represent the mean ± SE of nine individual experiments using cells isolated from three different donors. Statistical analysis was performed by Student's *t*-test, and statistical significance was taken as $P < 0.05$. N/S, not significant.

Phenotypic Regulation in Response to TGF-β1 Is Dependent on the Presence of the HA Pericellular Coat

Data presented above suggest that TSG-6-dependent regulation of the HA pericellular coat is required for TGF-β1 phenotypic conversion. However, TGF-β1 stimulation of HAS2-overexpressing cells and IL-1β stimulation in the aged phenotype suggest that the formation of the pericellular coat in itself does not lead to acquisition of a myofibroblastic phenotype. The role of the pericellular coat in TGF-β1-dependent regulation of phenotype was examined after its digestion with hyaluronidase (confirmed by particle exclusion) (Figure 12, C and D). There was no effect on TGF-β1-dependent induction of HAS2 (Figure 12A). In contrast, hyaluronidase digestion led to inhibition of TGF-β1-dependent phenotypic activation as determined by expression of α-SMA by Q-PCR (Figure 12B) and immunohistochemical analysis (Figure 12, E and F).

A   HAS2 mRNA

B

C   TSG-6 mRNA

D   α-SMA mRNA

Figure 10. HAS2 responsiveness is retained in aged cells after addition of IL-1β. Confluent monolayers of patient-matched young and aged dermal fibroblasts were growth-arrested in serum-free medium for 48 hours. The medium was then replaced with either serum-free medium alone (white bars), serum-free medium containing 10 ng/ml TGF-β1 (gray bars), or serum-free medium containing 1 ng/ml IL-1β (black bars) for a further 72 hours. mRNA was extracted, and cDNA prepared as described in *Materials and Methods*. HAS2 (**A**), TSG-6 (**C**), and α-SMA (**D**) expression was assessed by RT-QPCR. Ribosomal RNA expression was used as an endogenous control, and gene expression was assessed relative to control aged cells. The comparative C_T method was used for relative quantification of gene expression, and the results represent the mean ± SE of six individual experiments using cells isolated from two different donors. Statistical analysis was performed by Student's *t*-test and statistical significance was taken as $P < 0.05$. N/S, not Significant. **B:** HA secreted into the culture medium of aged cells was quantified by ELISA. Data are the mean ± SE of six individual experiments using cells isolated from two different donors. Statistical analysis was performed by Student's *t*-test: *$P < 0.05$; **$P < 0.01$, compared with control cells.

The relationship between assembly of a pericellular HA coat and cell surface CD44 has been well documented.[34–39] In our *in vitro* model of aging there were no age-related alterations in CD44 expression (data not
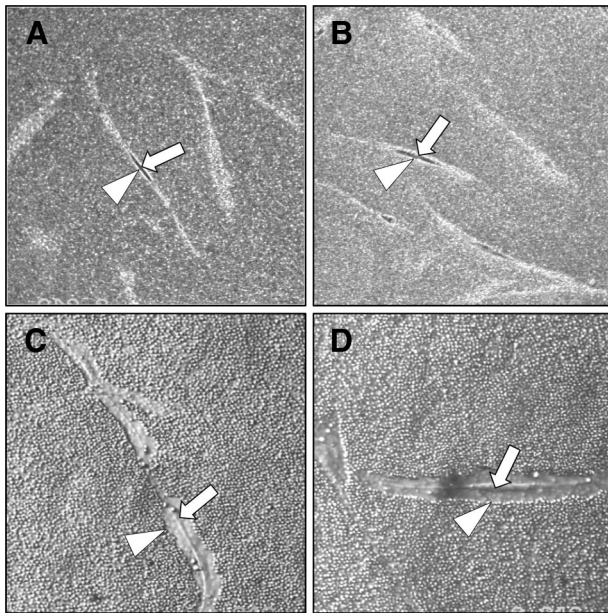
Figure 11. Effect of IL-1β on HA pericellular coat assembly. Subconfluent layers of patient-matched young (**A** and **C**) and aged (**B** and **D**) dermal fibroblasts were growth-arrested in serum-free medium for 48 hours. The medium was then replaced with either serum-free medium alone (**A** and **B**) or 1 ng/ml IL-1β (**C** and **D**) for 72 hours. Formalized horse erythrocytes were then added as described to visualize the HA pericellular coat. Zones of exclusion were visualized using a Zeiss Axiovert 135 inverted microscope. **Arrows** indicate the cell body; **arrowheads** show the extent of the pericellular matrix. Images are representative of dermal fibroblasts from two patient donors. Original magnification, ×200.

shown). We further examined the role of CD44 and the pericellular coat by inhibition of CD44 expression using siRNA. QPCR was used to confirm down-regulation of CD44 expression. It is of note that TGF-β1 itself decreased expression of CD44; however, CD44 siRNA resulted in a further reduction in expression both in unstimulated and TGF-β1-treated cells (Figure 12G). Consistent with the effects of inhibition of coat formation using hyaluronidase, suppression of CD44 expression was associated with abrogation of TGF-β1-dependent induction of α-SMA (Figure 12H).

Collectively these results suggest that the pericellular HA coat is therefore necessary but not sufficient to drive phenotypic fibroblast to myofibroblast activation.

Discussion

Impaired wound healing in elderly individuals is characterized by delayed re-epithelialization and an excessive inflammatory response, with the latter leading to matrix degradation by inflammatory cell-derived proteases.[40] It has been long established that there is marked alteration in fibroblast function with increasing age. In the normal aging human dermis, the fibroblast becomes a quiescent cell.[41] Fibroblast proliferation may also be modulated by age, resulting in decreased cell number at the wound site.[42] Aging in an *in vitro* model of wounding has also demonstrated a delay in the ability of human dermal fibroblasts to re-establish a confluent monolayer with increasing age.[43] Beyond the effects of aging on cellular

migration and proliferation, a loss of responsiveness to a variety of cytokines has been reported after *in vitro* and *in vivo* aging in human fibroblasts.[44,45]

The regulation of cellular phenotype and differentiation during tissue injury is an important determinant of wound-healing outcomes. In this context TGF-β1 is a key regulator of the wound-healing process as it is a key regulator of the fibroblast-myofibroblast phenotype. Myofibroblasts are responsible for closure of wounds and the formation of the collagen-rich scar. We have demonstrated previously that fibroblasts derived from nonscarring oral mucosa demonstrate intrinsic differences from donor-matched dermal fibroblasts in terms of their ability to differentiate into myofibroblasts.[23] More specifically, fibroblasts from the oral mucosa are resistant to TGF-β1-mediated phenotypic differentiation, which may in part explain the scar-free wound healing that occurs in the oral mucosa. In contrast, dermal fibroblasts readily differentiate into myofibroblasts and the linear polysaccharide, HA, plays a pivotal role in regulating this process of TGF-β1-driven cellular differentiation.

In the current study we show an age-dependent defect in myofibroblast phenotypic conversion, which may be of relevance to the impaired wound healing associated with aging. We subsequently sought to relate age-related changes in HA generation to this failure of phenotypic activation. The data clearly demonstrate a decrease in HA generation both in unstimulated cells and also after addition of TGF-β1 associated with *in vitro* aging. These data are consistent with our previous observations suggesting that increased HA generation was causally related to TGF-β1-mediated fibroblast-myofibroblast conversion.[23] Our previously published studies demonstrated a significant difference in HA generation under basal conditions with cells capable of myofibroblastic change, ie, young dermal fibroblasts, generating significantly more HA than fibroblasts resistant to phenotypic change, ie, oral mucosal fibroblasts.[23] Furthermore, we have demonstrated that the different basal patterns of HA generation were associated with the regulation of differing proliferative responses to TGF-β1 by the two fibroblast populations.[24] The data presented in the current study support a role for HA in dictating the cell's response to TGF-β1. We have demonstrated that *in vitro* aging is associated with a decrease in HA generation of dermal fibroblasts and attenuation of the hyaladherin TSG-6. In contrast, restoration of a high basal level of HA synthesis in the aged dermal fibroblast, as a result of HAS2 overexpression, resulted in restoration of TGF-β1-dependent induction of TSG-6. These data are also consistent with our recent studies in epithelial cells, which demonstrated that HA modulates TGF-β1 signaling after interaction with its receptor, CD44.[20,21]

In the current study *in vitro* aging and resistance to phenotypic conversion were accompanied by a failure of induction of HAS2 after addition of TGF-β1. Previously we demonstrated that resistance of oral mucosal fibroblasts to TGF-β1-mediated myofibroblastic change is also associated with failure of induction of HAS2. Moreover, silencing HAS2 gene expression using siRNA led to a significant inhibition of TGF-β1-dependent induction of
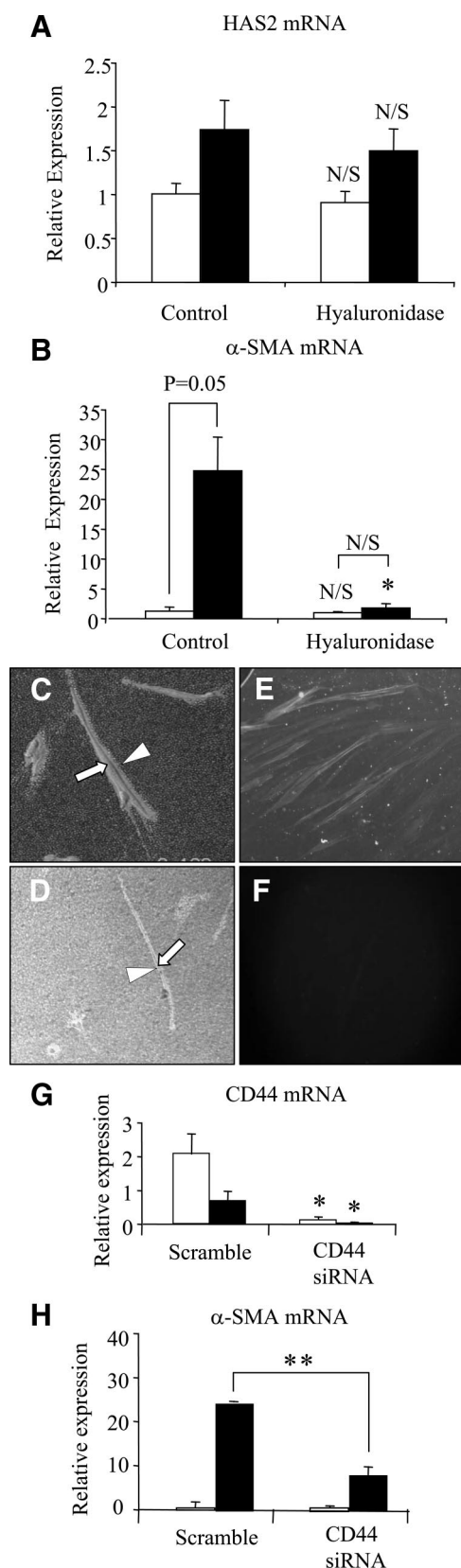
α-SMA. These observations led us to determine whether isoform-specific overexpression of HAS2 was sufficient to restore TGF-β1 responsiveness and phenotypic alteration in *in vitro* aged fibroblasts. Although overexpression of HAS2 was associated with increased HA generation, there was no alteration in α-SMA expression, suggesting that restoration of the age-dependent decrease in HAS2 expression was not the sole factor leading to the loss of TGF-β1-dependent phenotypic sensitivity. This finding is consistent with the observation that the aged cells retained the ability to induce HAS2 in response to IL-1β, suggesting that aging specifically affects TGF-β1 responses rather than causing a global defect in HAS2 regulation.

Many studies have demonstrated the importance of HA-binding proteins, termed hyaladherins, in the organization of HA matrices. One hyaladherin that has a particular role in the formation of pericellular HA coats is TSG-6. Fülöp et al[31] have shown that TSG-6^{−/−} mice are infertile because of their inability to form HA-rich extracellular matrix. In addition, we have also previously shown the importance of TSG-6 in the formation of a pericellular HA in epithelial cells of renal origin.[33] In the current study we have demonstrated an age-dependent decrease in TSG-6 expression both in unstimulated cells and also after stimulation by TGF-β1. Furthermore, silencing of TSG-6 gene expression using siRNA led to an inhibition

Figure 12. Consequences of inhibiting HA coat assembly on TGF-β1-dependent phenotypic activation of fibroblasts. Confluent monolayers of young dermal fibroblasts were growth-arrested in serum-free medium for 48 hours. Bovine testicular hyaluronidase (200 μg/ml) was then added in serum-free medium at 37°C for 1 hour before the addition (to the hyaluronidase) of either serum-free medium alone (white bars) or 10 ng/ml TGF-β1 (black bars) for a further 72 hours. In control experiments hyaluronidase treatment was replaced by adding serum-free medium alone. HAS2 (**A**) and α-SMA (**B**) mRNA expression was assessed by RT-QPCR. Ribosomal RNA expression was used as an endogenous control, and gene expression was assessed relative to the control treatment in nonstimulated cells. The comparative C$_T$ method was used for relative quantification of gene expression, and the results represent the mean ± SE of six individual experiments using cells isolated from two different donors. Statistical analysis was performed by the Student's *t*-test: *$P < 0.05$, compared with control treatment; N/S, not significant. In parallel experiments, serum-free medium alone (**C**) or bovine testicular hyaluronidase (200 μg/ml) (**D**) were added to growth-arrested cells for 1 hour before the addition of 10 ng/ml TGF-β1, and the incubations were continued for 72 hours. Formalized horse erythrocytes were then added to visualize the HA pericellular coat. Zones of exclusion were visualized using a Zeiss Axiovert 135 inverted microscope. **Arrows** indicate the cell body; **arrowheads** show the extent of the pericellular matrix. Images are representative of dermal fibroblasts from two patient donors. Original magnification, ×200. Immunohistochemical analysis was also performed to assess dermal fibroblast phenotype after treatment with hyaluronidase. Serum-free medium alone (**E**) or bovine testicular hyaluronidase (200 μg/ml) (**F**) was added to growth arrested cells for 1 hour before the addition of 10 ng/ml TGF-β1, and the incubations were continued for 72 hours. The cells were fixed and stained for α-SMA, mounted in Vectashield fluorescent mountant, and viewed under UV light. Original magnification, ×100. The relationship between the pericellular coat and regulation of the cell phenotype was also examined by CD44 gene silencing (**G** and **H**). Total mRNA was extracted from young dermal fibroblasts after transfection with CD44 siRNA or scrambled oligonucleotide control (scramble) and incubated in medium supplemented with 10% FBS for 24 hours. The medium was then replaced with serum-free medium for a further 24 hours, before addition of serum-free medium alone (white bars) or serum-free medium containing 10 ng/ml TGF-β1 (black bars) for 72 hours. CD44 (**G**) and α-SMA (**H**) expression was assessed by RT-QPCR. Ribosomal RNA expression was used as an endogenous control and gene expression was assessed relative to control-scrambled samples. The comparative C$_T$ method was used for relative quantification of gene expression, and the results represent the mean ± SE of six individual experiments using cells isolated from two different donors. Statistical analysis was performed by Student's *t*-test: *$P < 0.05$; **$P < 0.01$, compared with scramble.

of TGF-β1-dependent induction of α-SMA. This result suggests that coordinated induction of HAS2 and TSG-6 facilitation of HA pericellular coat assembly are necessary to allow TGF-β1-dependent phenotypic activation of fibroblasts, and both components of this response are impaired with aging.

The importance of the pericellular HA coat in regulating the fibroblast-myofibroblast activation process is further highlighted by the data demonstrating that inhibition of coat formation by hyaluronidase enzymatic action or CD44 gene silencing also prevented TGF-β1-mediated phenotypic conversion. In contrast, however, formation of a pericellular coat after stimulation with IL-1β did not facilitate phenotypic activation. Similarly stimulation of HAS2-overexpressing cells, although restoring the cell's ability to form a pericellular coat, was not associated with phenotypic activation. These data therefore suggest that, although necessary for TGF-β1-dependent phenotypic activation, formation of the coat in itself is not the sole driving force and is not sufficient to drive the myofibroblastic phenotype.

Understanding regulation of the fibroblast phenotype has implications in terms of regulation of tissue fibrosis beyond the context of wound healing. Progressive fibrosis of superficial tissues and internal organs can result in an array of clinical conditions ranging from disfigurement and progressive disability to end-stage organ failure and death. Fibrosis is a key component of numerous chronic diseases including pulmonary fibrosis, chronic kidney disease, liver cirrhosis, and congestive cardiac failure, well known causes of death and disability worldwide.[46–50] Fibrosis can be considered as a form of aberrant wound healing in which there is progression rather than resolution of scarring. It results from unabated myofibroblast activity leading to excessive accumulation of extracellular matrix causing disruption of normal tissue architecture and function. The identification of HA as a key component of the regulatory mechanism that dictates the phenotypic response of a fibroblast both in our previous studies of patient-matched oral and dermal fibroblasts and in the current model of *in vitro* aging therefore suggests this may be a common mechanism regulating fibroblast behavior in a much wider context.

In summary, the data presented demonstrate an age-related alteration in fibroblast behavior, which results in an inability to undergo phenotypic transformation to become a myofibroblast. This failure may have a direct implication in impaired wound healing associated with aging. Our data add further support to the hypothesis that the matrix polysaccharide HA is an important component of the regulation of fibroblast phenotype and that its dysregulation may be casually related to failure of a fibroblast to acquire a myofibroblastic phenotype. Finally, the data suggest that organization of HA into a pericellular coat is necessary for the activation of fibroblasts to myofibroblasts, but that formation of the coat in itself does not lead to phenotypic activation and restoration of coat formation in aging cells is not sufficient to restore the failure of phenotypic activation of fibroblasts associated with aging.

References

1. Ashcroft GS, Mills SJ, Ashworth JJ: Aging and wound healing. Biogerontology 2002, 3:337–345
2. Ashcroft GS, Roberts AB: Loss of Smad3 modulates wound healing. Cytokine Growth Factor Rev 2000, 11:125–131
3. Gabbiani G: The myofibroblast in wound healing and fibrocontractive diseases. J Pathol 2003, 200:500–503
4. Desmoulière A, Darby IA, Gabbiani G: Normal and pathologic soft tissue remodeling: the role of the myofibroblast, with special emphasis on liver and kidney fibrosis. Lab Invest 2003, 83:1689–1707
5. Tomasek JJ, Gabbiani G, Hinz B, Chaponnier C, Brown RA: Myofibroblasts and mechano-regulation of connective tissue remodelling. Nat Rev Mol Cell Biol 2002, 3:349–363
6. Eddy AA: Progression in chronic kidney disease. Adv Chronic Kidney Dis 2005, 12:353–365
7. Schuppan D, Koda M, Bauer M, Hahn EG: Fibrosis of liver, pancreas and intestine: common mechanisms and clear targets? Acta Gastroenterol Belg 2000, 63:366–370
8. Desmoulière A, Geinoz A, Gabbiani F, Gabbiani G: Transforming growth factor β1 induces α-smooth muscle actin expression in granulation tissue myofibroblasts and in quiescent and growing cultured fibroblasts. J Cell Biol 1993, 122:103–111
9. Evans RA, Tian YC, Steadman R, Phillips AO: TGF-β1-mediated fibroblast-myofibroblast terminal differentiation-the role of Smad proteins. Exp Cell Res 2003, 282:90–100
10. Mogford JE, Tawil N, Chen A, Gies D, Xia Y, Mustoe TA: Effect of age and hypoxia on TGFβ1 receptor expression and signal transduction in human dermal fibroblasts: Impact on cell migration. Cell Physiol 2002, 190:259–265
11. Spicer AP, Kaback LA, Smith TJ, Seldin MF: Molecular cloning and characterization of the human and mouse UDP-glucose dehydrogenase genes. J Biol Chem 1998, 271:25117–15124
12. Spicer AP, McDonald JA: Characterisation and molecular evolution of a vertebrate hyaluronan synthase gene family. J Biol Chem 1998, 272:1923–1932
13. Kosaki R, Watanabe K, Yamaguchi Y: Overproduction of hyaluronan by expression of the hyaluronan synthase Has2 enhances anchorage independent growth. Cancer Res 1999, 59:1141–1145
14. Itano N, Atsumi F, Sawai T, Yamada Y, Miyaishi O, Senga T, Hamaguchi M, Kimata K: Abnormal accumulation of hyaluronan matrix diminishes contact inhibition of cell growth and promotes cell migration. Proc Natl Acad Sci USA 2002; 99:3609–3614
15. Ito T, Williams JD, Al-Assaf S, Phillips GO, Phillips AO: Hyaluronan and proximal tubular epithelial cell migration. Kidney Int 2004, 65:823–833
16. Legg JW, Lewis CA, Parsons M, Ng T, Isacke CM: A novel PKC-regulated mechanism controls CD44 ezrin association and directional cell motility. Nat Cell Biol 2002, 4:399–407
17. Zoltan-Jones A, Huang L, Ghatak S, Toole BP: Elevated hyaluronan production induces mesenchymal and transformed properties in epithelial cells. J Biol Chem 2003, 278:45801–45810
18. Brecht M, Mayer U, Schlosser E, Prehm P: Increased hyaluronate synthesis is required for fibroblast detachment and mitosis. Biochem J 1986, 239:445–450
19. Evanko SP, Angello JC, Wight TN: Formation of hyaluronan- and versican-rich pericellular matrix is required for proliferation and migration of vascular smooth muscle cells. Arterioscler Thromb Vasc Biol 1999, 19:1004–1013
20. Ito T, Williams JD, Fraser DJ, Phillips AO: Hyaluronan attenuates TGF-β1 mediated signalling in renal proximal tubular epithelial cells. Am J Pathol 2004, 164:1979–1988
21. Ito T, Williams JD, Fraser DJ, Phillips AO: Hyaluronan regulates TGF-β1 receptor compartmentalization. J Biol Chem 2004, 279:25326–25332
22. Jenkins RH, Thomas GJ, Williams JD, Steadman R: Myofibroblastic differentiation leads to hyaluronan accumulation through reduced hyaluronan turnover. J Biol Chem 2004, 279:41453–41460
23. Meran S, Thomas D, Stephens P, Martin J, Bowen T, Phillips A, Steadman R: Involvement of hyaluronan in regulation of fibroblast phenotype. J Biol Chem 2007, 282:25687–25697
24. Meran S, Thomas DW, Stephens P, Enoch S, Martin J, Steadman R, Phillips AO: Hyaluronan facilitates transforming growth factor-β1-mediated fibroblast proliferation. J Biol Chem 2008, 283:6530–6545
25. Vigetti D, Viola M, Karousou E, Rizzi M, Moretto P, Genasetti A, Clerici

M, Hascall VC, De Luca G, Passi A: Hyaluronan-CD44-ERK1/2 regulate human aortic smooth muscle cell motility during aging. J Biol Chem 2008, 283:4448–4458

26. Vigetti D, Moretto P, Viola M, Genasetti A, Rizzi M, Karousou E, Pallotti F, De Luca G, Passi A: Matrix metalloproteinase 2 and tissue inhibitors of metalloproteinases regulate human aortic smooth muscle cell migration during in vitro aging. FASEB J 2006, 20:1118–1130

27. Shiraha H, Gupta K, Drabik K, Wells A: Aging fibroblasts present reduced epidermal growth factor (EGF) responsiveness due to preferential loss of EGF receptors. J Biol Chem 2000, 275:19343–19351

28. Ashcroft GS, Horan MA, Ferguson MW: The effects of aging on cutaneous wound healing in mammals. J Anat 1995, 187:1–26

29. Stephens P, Davies KJ, Occleston N, Pleass RD, Kon C, Daniels J, Khaw PT, Thomas DW: Skin and oral fibroblasts exhibit phenotypic differences in extracellular matrix reorganization and matrix metalloproteinase activity. Br Journal Dermatol 2001, 144:229–237

30. Cristofalo VJ, Allen RG, Pignolo RJ, Martin BG, Beck JC: Relationship between donor age and the replicative lifespan of human cells in culture: a reevaluation. Proc Natl Acad Sci USA 1998, 95:10614-10619

31. Fülöp C, Szanto S, Mukhopadhyay D, Bardos T, Kamath RV, Rugg MS, Day AJ, Salustri A, Hascall VC, Glant TT, Mikecz K: Impaired cumulus mucification and female sterility in tumor necrosis factor-induced protein-6 deficient mice. Development 2003, 130:2253–2261

32. Rugg MS, Willis AC, Mukhopadhyay D, Hascall VC, Fries E, Fülöp C, Milner CM, Day AJ: Characterization of complexes formed between TSG-6 and inter-α-inhibitor that act as intermediates in the covalent transfer of heavy chains on to hyaluronan. J Biol Chem 2005, 280:25674–25686

33. Selbi W, Day AJ, Rugg MS, Fülöp C, de la Motte CA, Bowen T, Hascall VC, Phillips AO: Overexpression of hyaluronan synthase 2 alters hyaluronan distribution and function in proximal tubular epithelial cells. J Am Soc Nephrol 2006, 17:1553–1567

34. Oertli B, Fan X, Wüthrich RP: Characterization of CD44-mediated hyaluronan binding by renal tubular epithelial cells. Nephrol Dial Transplant 1998, 13:271–278

35. Lüke HJ, Prehm P: Synthesis and shedding of hyaluronan from plasma membranes of human fibroblasts and metastatic and non-metastatic melanoma cells. Biochem J 1999, 343:71–75

36. Tammi R, MacCallum D, Hascall VC, Pieninäkit JP, Hyttinen M, Yammi M: Hyaluronan bound to CD44 on keratinocytes is displaced by hyaluronan decasaccharides and not hexasaccharides. J Biol Chem 1998, 273:28878–28888

37. Nandi A, Esress P, Siegelman MH: Hyaluronan anchoring and regulation on the surface of vascular endothelial cells is mediated through the functionally active form of CD44. J Biol Chem 2000, 275:14939–14948

38. Heldin P, Pertoft H: Synthesis and assembly of the hyaluronan-containing coats around normal human mesothelial cells. Exp Cell Res 1993, 208:422–429

39. Lesley J, Hascall VC, Tammi M, Hyman R: Hyaluronan binding by cell surface CD44. J Biol Chem 2000, 275:26967–26975

40. Ashcroft GS, Horan MA, Ferguson MW: Aging alters the inflammatory and endothelial cell adhesion molecule profiles during human cutaneous wound healing. Lab Invest 1998, 78:47–58

41. Pieraggi MJ, Bouissou H, Angelier C, Uhart D, Magnol J, Kokolo J: Le fibroblaste. Ann Pathol 1985, 5:65–76

42. Bruce SA, Deamond SF: Longitudinal study of in vivo wound repair and in vitro cellular senescence of dermal fibroblasts. Exp Gerontol 1991, 26:17–27

43. Muggleton-Harris AL, Reisert PS, Burghoff RL: In vitro characterization of response to stimulus (wounding) with regard to aging in human skin fibroblasts. Mech Aging Dev 1982, 19:37–43

44. Matrisian LM, Davis D, Magun BE: Internalization and processing of epidermal growth factor in aging human fibroblasts in culture. Exp Gerontol 1987, 22:81–89

45. Rattan SI, Derventzi A: Altered cellular responsiveness during aging. BioEssays 1991, 13:601–601

46. Bedossa P, Paradis V: Liver extracellular matrix in health and disease. J Pathol 2003, 200:504–515

47. Chapman HA: Disorders of lung matrix remodeling. J Clin Invest 2004, 113:148–157

48. Eddy AA: Molecular basis of renal fibrosis. Pediatr Nephrol 2000, 15:290–301

49. Francis GS, McDonald K, Chu C, Cohn JN: Pathophysiologic aspects of end-stage heart failure. Am J Cardiol 1995, 75:11A–16A

50. Green FHY: Overview of pulmonary fibrosis. Chest 2002, 122:334S–339S